Acta Cryst. (1957). **10**, 149

The Structure of Chrysotile. V. Diffuse Reflexions and Fibre Texture

By E. J. W. Whittaker

Ferodo Limited, Chapel-en-le-Frith, Stockport, England

(*Received 9 October* 1956)

The distributions of intensity in a number of diffuse chrysotile reflexions are calculated on the basis of the cylindrical structure described in previous papers. It is shown that these intensity distributions are profoundly affected by the presence of a distribution of fibril diameters, and a plausible type of probability function is introduced to serve as a basis for calculation. Comparison of the observed and calculated intensity curves then permits the derivation of reasonable values of the statistical parameters, the radius of the strain-free layer and the *b* parameter of the cylindrical lattice. The effect of spiral, helical, and incomplete cylindrical layers is discussed in relation both to the X-ray diffraction pattern and to the density of chrysotile.

1. Introduction

The investigation of the details of the structure of the three varieties of chrysotile described in the preceding parts of this series (Whittaker, 1953, 1956*a*, *b*, *c*) has been based on the sharp reflexions, and the diffuse 0*kl* reflexions have been used only as qualitative evidence in favour of a partly disordered layer structure. However, for a structure analysis of chrysotile to be completely acceptable it must give a satisfactory explanation of the diffuse reflexions.

Jagodzinski & Kunze (1954*a*) have calculated the intensity distributions in certain of these reflexions on the basis of a cylindrical layer structure. Their calculations lead to theoretical intensity curves with principal maxima in the observed positions, and agree with observation in so far as both calculated and observed intensity curves for 011, 020, 031, 040, and 051 have long 'tails' and those for 060 do not, while those for 033 are of a somewhat intermediate character. Their calculated curves differ from the observed ones, however, in that they exhibit along the 'tails' of the reflexions many marked maxima and minima of intensity which are never observed on X-ray diffraction photographs. The authors correctly ascribe the cause of this discrepancy to the fact that no allowance was made in the calculations for a distribution of fibre diameters.

In the present work the reflexions 011, 013, 031, 033, 060 and 062 are discussed in some detail, and the conditions are investigated under which the unobserved maxima and minima are suppressed.

2. Theoretical and procedural considerations

It has been shown (Whittaker, 1955*a*) that the intensity scattered by a regular cylindrical structure into diffuse reflexions on the *l*th layer line is given by

$$I(\xi, l) = \frac{2Q^2}{R^2} \sum_m \sum_K p_m^2 \left\{ \left| \sum_j f_j \exp\left[2\pi i l \frac{z_j}{c}\right] \times J_{Kp_m}\left(p_m \frac{b_{m,j}}{b} k\right) \cos 2\pi \frac{Ky_j}{b} \right|^2 + \left| \sum_j f_j \exp\left[2\pi i l \frac{z_j}{c}\right] J_{Kp_m}\left(p_m \frac{b_{m,j}}{b} k\right) \sin 2\pi \frac{Ky_j}{b} \right|^2 \right\}. \quad (1)$$

The summations extend over the layers of the structure (m), the atoms in the structural unit of a layer (j). and the positive integers K. The symbols used have the following meanings:

Q	is the X-ray scattering function for an electron,
R	is the distance of the point of observation from the specimen,
p_m	is the number of repeating units in the circumference of the mth layer,
f_j	is the scattering factor of the jth atom,
x_j, z_j	are the radial and axial cylindrical co-ordinates of the jth atom, referred to an arbitrary origin in the neutral surface of the layer with respect to bending,
$y_{m,j}$	is the arcual distance of the jth atom in the mth layer from an initial radial plane,
$b_{m,j}$	is the value of $y_{m,j}$ after which the structure repeats (at the radial co-ordinate x_j in the mth layer),
b	is the value of $b_{m,j}$ on the neutral surface of the layer with respect to bending,
y_j	is defined by the relation $y_j/b = y_{m,j}/b_{m,j}$,
k	is the index of reflexion in reciprocal space regarded as a continuous variable, i.e. $k = \xi b/\lambda$.

In the derivation of this formula the innermost layer of the structure was assumed to have a radius a_0, and the mth layer to have a radius a_0+ma. In the present discussion it will be convenient to change the origin of the ordinal number m so that the mth layer is of radius ma. The lower limit of the summation over m is then non-zero. The values of m may also be non-integral, but there is no significant difference in the results of the calculations if only integral values of m are considered, since the use of non-integral values would only involve changes of up to ±3·7 Å in the assumed value of the radius of the innermost layer of the structure.

It has been shown in earlier papers of this series (Whittaker, 1953, 1956*a*, *b*) that in the structure of chrysotile alternate layers are either relatively displaced parallel to the z axis, as in clino-chrysotile, or are equivalent after reversal in the directions of the y and z axes. Neither of these changes has any effect on (1). In clino-chrysotile there is evidence of small distortions of the structure in opposite directions in alternate layers, but it has been shown that distortions of the atomic positions of this order of magnitude have a negligible effect on the results calculated from (1) for low-order reflexions. In computing the profiles of the diffuse reflexions from (1) we may therefore regard all the layers as equivalent, and we may use the halved value of a (7·3 Å). Since the positions and form of the diffuse reflexions are independent of the angle β it is also convenient to express the atomic positions in terms of orthogonal coordinates. It is assumed that the neutral surface of the layers with respect to bending lies at the junction of the silicate and brucite half-layers, and passes through the O_3 atoms; i.e. the parameter b is assumed to be the repeat distance defined by the net of O_3 atoms. The possibility of an error in this assumption is discussed in § 7.

The parameters of the cylindrical lattice of clino- and ortho-chrysotile have been shown (Whittaker, 1956*a*, *b*) to be

$$a \sin \beta = 14{\cdot}63, \quad b \simeq 9{\cdot}2, \quad c = 5{\cdot}34 \text{ Å},$$

with $\beta = 93° 16'$ for clino-chrysotile and $\beta = 90°$ for ortho-chrysotile. The fractional co-ordinates of the atoms which have been assumed are shown in Table 1. The x and z co-ordinates have been obtained from the results of Part II (Whittaker, 1956*a*) by the appropriate transformation of axes, change of origin, and halving of the a axis. The y co-ordinates have been chosen to give the maximum regularity of the atomic positions in a kaolin-like layer. The cylindrical projection of this layer on (100) has the two-dimensional space group a $1m1$, which is in accordance with the considerations advanced in Part II, and is in fact the only one of the three possible space groups for this projection which is compatible with the z coordinates deduced in that paper. The equivalent positions in this space group are:

Fourfold: $y, z;\ \bar{y}, z;\ \tfrac{1}{2}+y, \tfrac{1}{2}+z;\ \tfrac{1}{2}-y, \tfrac{1}{2}+z$.
Twofold: $0, z;\ \tfrac{1}{2}, \tfrac{1}{2}+z$.

Table 1. *Atomic co-ordinates in a single layer referred to orthogonal axes, with the a axis halved*

The values are derived from the results for clino-chrysotile; the value of z/c for O_1 is taken as the mean of the values in alternate layers in that structure

	x/a	y/b	z/c
O_1	−0·326	0	+0·025
O_2	−0·300	+0·250	+0·273
Si	−0·234	+0·167	+0·024
O_3	0	+0·167	+0·023
OH_1	0	+0·500	+0·023
Mg_1	+0·154	+0·500	+0·361
Mg_2	+0·154	+0·167	+0·361
OH_2	+0·284	0	+0·196
OH_3	+0·284	+0·333	+0·196

When these values are inserted in expression (1) the terms involving sin $(2\pi K y_j/b)$ disappear. It may also be noted that the two O_2 atoms lie on a cylindrical lattice with the b parameter reduced by a factor of 2, and that the O_3+OH_1, the Mg_1+Mg_2, and the OH_2+OH_3 atoms severally lie on cylindrical lattices with the b parameter reduced by a factor of 3. The most convenient form of (1) for computation is thus, for a given value of K,

$$I(\xi, l) = \frac{8Q^2}{R^2} \sum_m p_m^2 \left| \sum_j u_j f_j \exp\left[2\pi i l \frac{z_j}{c}\right] \times \cos 2\pi \frac{K y_j}{b} J_{Kp_m}\left(p_m \frac{b_{m,j}}{b} k\right)\right|^2, \quad (2)$$

where u_j is the multiplicity of the jth atom with respect to the reflexion of order K. The values of u_j are

$u_{O_1} = 1,\ u_{Si} = 2$ for all reflexions,
$u_{O_2} = 2$ for $K = 2n$ and zero for $K = 2n+1$,

and the remaining u_j values are 3 for $K = 3n$ and zero otherwise.

In order to perform the computations, graphs of $J_{Kp_m}(p_m k')$ were prepared for the required values of K and m from the data given by Jahnke & Emde (1952). The appropriate values of the Bessel functions were then interpolated from these graphs after calculation of tables of $b_{m,j}k/b$ for all the atoms and for all relevant values of m. In certain cases the calculations were abbreviated by omitting altogether the terms with alternate values of m. This procedure is permissible in the vicinity of $k = K$ (i.e. $k < 1{\cdot}5K$), where $J_{Kp_m}(p_m k)$ is a slowly varying function of m; it is not permissible when $k \gg K$. For the sake of simplicity the f values of all the atoms were taken to have the values appropriate at the integral lattice point $k = K$ for each reflexion, and a mean functional dependence on ξ was assumed over the region of reciprocal space for which the reflexion profile was calculated. This permitted the f values to be treated as constants during each calculation, and their variation could then be allowed for after all the summations had been performed.

In most cases only terms having K equal to the index of the nearest reciprocal-lattice point were taken into account in the computation. In the case of the 031 reflexion, however, the effect of terms with $K = 1$ (i.e. the 'tail' of the 011 reflexion) was considered and it was shown to have a negligible effect on the 031 profile.

In a previous paper (Whittaker, 1955*a*) there were presented the results of calculations of the profiles of $0kl$ reflexions from a cylindrical lattice with scattering matter concentrated at the lattice points. These results were presented after multiplying the equation corresponding to (1) by the variable k in order to make the integrated intensity under the curve between any arbitrary values of k equal to that recorded between the corresponding points on a film after correction by the Lorentz factor. This procedure was carried over from the earlier work on the sharp reflexions, but it is not the most appropriate method for comparing calculated and observed diffuse reflexions. In the present work the curve calculated from (1) is compared with the observed densitometer record after the latter has been corrected for polarization, absorption, and Cox & Shaw factors, and has been replotted on an abscissa scale linear in k.

3. Evidence for a distribution of fibril sizes

The first computations were carried out for the reflexion 011. Only the O_I and Si atoms contribute to this reflexion, and as these atoms have closely similar values of $b_{m,j}/b$ and z_j/c, and the same signs of $\cos 2\pi K y_j/b$, the general shape of the reflexion is very similar to a diffuse reflexion from a cylindrical lattice with scattering matter concentrated at the lattice points. Fig. 1, curve (*b*), shows the profile calculated for the 011 reflexion from a rotated chrysotile fibril (or a bundle of equal fibrils) containing thirteen layers and having internal and external radii of $6a$ and $18a$ ($a = 7{\cdot}3$ Å). This differs from the observed reflexion (curve (*a*)) in two principal ways: (i) the 'tail' of the calculated reflexion contains an oscillatory component, which is never observed; (ii) the principal maximum falls off more rapidly on the high-angle side than on the low-angle side, whereas the converse is true of the observed reflexion.

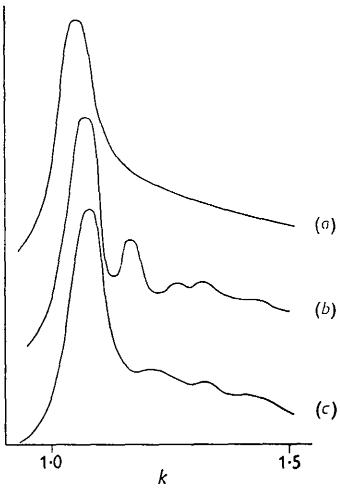

Fig. 1. Profile of the 011 reflexion: (*a*) observed; (*b*) calculated for a single fibril; (*c*) calculated for a specimen containing a distribution of fibril sizes based on an exponential function of the strain energy involved in the curvature of the layers.

The oscillatory component of the 'tail' arises from the oscillations of the Bessel functions which describe the contributions from each layer of the structure. These contributions fall to zero at each oscillation in the reflexion from a cylindrical lattice, and very nearly to zero in the case of the 011 reflexion from chrysotile, but the positions of the oscillations in these contributions are functions of the radii of the layers. The result is that the oscillations arising from the intermediate layers are largely smoothed out, but there is a residual oscillatory component which arises predominantly from the contributions of the innermost and outermost layers. The effect is reduced, though not eliminated, if these two layers are assigned a statistical weight lower than that of the other layers.

In view of the considerations advanced above it is reasonable to suppose that the oscillatory component would be more satisfactorily suppressed if all the layers of the structure were assigned statistical weights falling smoothly to zero as their radii increase or decrease from some mean value. Such a distribution of statistical weights is also very reasonable on physical grounds, since only one layer in a chrysotile fibril can be bent to the radius at which it is strain free; all other layers will be subject to a degree of strain which increases as the radius increases or decreases from this optimum, and they may be expected to occur less frequently as the strain increases.

If the brucite-like and silicate half-layers are assumed to be replaced by elastic laminae it may be shown that the total strain energy in unit length of the mth complete cylindrical layer of radius ma ($a = 7{\cdot}3$ Å) is proportional to

$$m(1/m - 1/m_0)^2$$

if the m_0th layer is strain free.* If we assume that the strain-free layer is formed first and the fibre grows inwards and outwards from this layer, and that the probability of formation of the mth layer depends jointly on an exponential function of the strain energy and on the probability of the prior existence of the appropriate substrate layer (the $(m-1)$th or $(m+1)$th, according as $m \gtrless m_0$), then the statistical weight of the mth layer may be shown to be of the form

---

* The parameter m need not be integral but is subject to the condition $5m =$ an integer; also m_0 need not necessarily be a permitted value of m, since it is conceivable that no layer of the structure is wholly strain free, but this does not involve any fundamental change in the theory.

$$\left.\begin{aligned} &\prod_{m_0}^{m} \exp\left\{-tm\left(\frac{1}{m}-\frac{1}{m_0}\right)^2\right\} \qquad m > m_0 \\ \text{and}\qquad &\prod_{m}^{m_0} \exp\left\{-tm\left(\frac{1}{m}-\frac{1}{m_0}\right)^2\right\} \qquad m < m_0\,, \end{aligned}\right\} \qquad (3)$$

where t is an undetermined constant.

Fig. 1, curve (*c*), shows the profile of 011 calculated on the assumption of a frequency distribution of layer diameters based on the above formulae with $m_0 = 9$ and $t = 10$. Comparison of this curve with curve (*b*) demonstrates the effectiveness of this method in eliminating the oscillatory component of the tail.

4. Evidence for layer boundaries

Of the two principal discrepancies between the calculated and observed profiles of 011, the excessive sharpness of the main peak on the high-angle side relative to that on the low-angle side is not alleviated very much by the introduction of the exponential weighting function. It can be alleviated by weighting functions which assign high statistical weights to layers of the smallest radii. However, such an assumption appears to be physically unlikely, and in any case it leads to excessive breadth on the low-angle side and to poor suppression of the oscillatory component of the tail. Three other possible explanations of the discrepancy have therefore been considered:

(*a*) Distortions of the structure. If the atoms do not have exactly the y co-ordinates given in Table 1 some of the atoms other than O_1 and Si may provide small contributions to the 011 reflexion, and these could conceivably modify the profile in the required sense. In order to introduce reasonable mutually consistent distortions of the structure it was assumed that the SiO_4 tetrahedra might suffer small rigid rotations about the (orthogonal) x and z axes, and that the relative displacements of the other atoms would then be appropriate to a packing of spheres. The 011 reflexion profile was therefore calculated for a hypothetical structure containing such a set of mutually consistent displacements with a maximum atomic displacement of 0·2 Å. No improvement was achieved, however, and this conclusion was confirmed by similar calculations on 013.

(*b*) The helical cylindrical lattice. The sharpness of the high-angle side of the calculated peak is due to the deep and almost coincident first minima in the functions which define the contributions from the individual layers of the structure. It has been shown (Whittaker, 1955*d*) that the depth of these minima is reduced if the cylindrical lattice is helical instead of regular. However, this cannot be invoked as the principal factor responsible for the discrepancy, since the latter is not appreciably greater in the case of the 011 reflexion from the specimen studied in Part II (Whittaker, 1956*a*), which is known to be predominantly helical,than in the case of the specimen studied in Part III (Whittaker, 1956*b*), which is known to be predominantly non-helical.

(*c*) Layer boundaries. It has been shown by optical diffraction (Whittaker, 1955*b*) that rotated spiral and incomplete circular lattices give diffuse reflexions similar to those from circular lattices, except for a diminution of the depth of the first minimum. It is therefore suggested that the observed 011 profile of chrysotile can be explained either if the fibres have a spiral cylindrical lattice, or if there are present both circular cylindrical structures and incomplete bounded layers in the form of cylindrical arcs. For reasons which are discussed in § 7, the latter explanation is preferred.

5. Comparison of observed and calculated results

Fig. 2 shows a comparison of the observed and calculated profiles of the six reflexions studied. In order to facilitate comparisons of shape, the observed profiles are drawn to various convenient scales and the calculated curves have been scaled in each case to the same peak heights as those observed; the actual peak intensities have a disagreement factor $\Sigma|I_o - I_c| \div \Sigma I_0 =$ 0·19. As this corresponds to a value of about 0·09 for

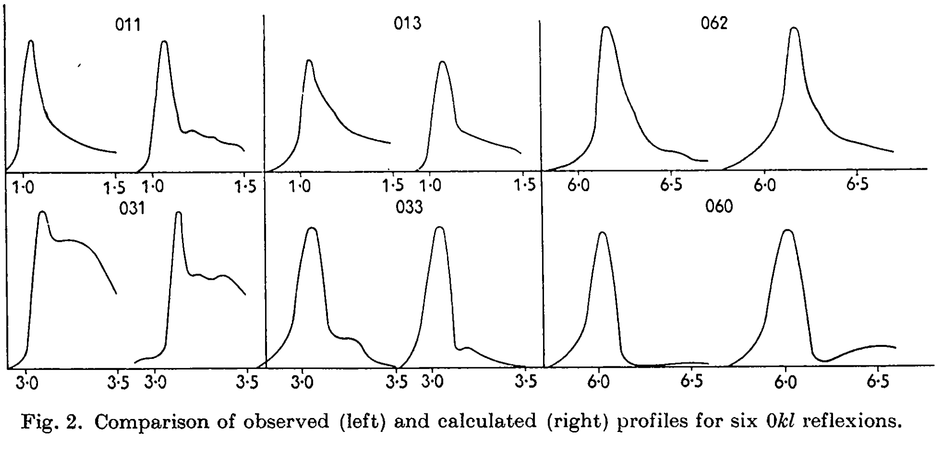

Fig. 2. Comparison of observed (left) and calculated (right) profiles for six $0kl$ reflexions.

the usual factor based on amplitudes, it is reasonably satisfactory in spite of the small number of reflexions considered. The calculated curves in Fig. 2 are all based on the exponential statistical weight function discussed in § 3 with $m_0 = 9$ and $t = 10$. These values were chosen, from a number of trials, to give about the right spread of layer sizes in order to give reasonably satisfactory 011 and 031 profiles.

The general comparison of reflexion shapes is satisfactory. In particular, the secondary maxima following the main peaks of the 031, 033, and 060 reflexions are reproduced by the calculations, and this makes it understandable that Aruja (1943) should have had difficulty in indexing these secondary maxima. The peculiar shape of 060 with its diffuse low-angle 'toe' and sharp cut-off towards high angles is also reproduced, as are its relative sharpness and its very small displacement from the integral reciprocal-lattice point. The last features confirm that Aruja's assumption of step-wise displacement disorder in steps of $b/6$ is unnecessary, as Jagodzinski & Kunze (1954*a*) have already pointed out.

Apart from the excessively sharp high-angle side of 011 and 013, which has been discussed in § 4, the two main discrepancies in the general shape of the curves are the low subsidiary maximum calculated for 031 and the high subsidiary maximum calculated for 060. It has been shown that the former discrepancy is not alleviated by varying the assumed layer-diameter distribution nor by introducing the structural distortions discussed in § 4(*a*). It has been found that the subsidiary maximum following 060 is reduced if the assumed diameters are increased. There is other evidence (discussed below) that the assumed diameters are too small, but it is doubtful whether a reasonable change would eliminate the discrepancy. It has not been possible to assess the effect of layer boundaries on these two reflexions.

The observed reflexions are generally sharper on the low-angle side than are the calculated profiles, which shows that the assumed diameters are too small. This question is discussed quantitatively in § 6.

6. The size of the fibrils

The diameters of the layers which compose the fibrils can be assessed in two independent ways: from the sharpness of the $0kl$ reflexions on the low-angle side and from the displacement of the maxima of certain of them.

It is found that the gradient of the calculated profile of an $0kl$ reflexions at any point on the low-angle side of the peak is approximately the same as that of the function $J^2_{kp_{\bar{m}}}(kp_{\bar{m}})$ for the $\bar{m}$th layer, where $\bar{m}$ is the value of m at the maximum value of $T_m p^2_{\bar{m}}$, T_m being the statistical weight of the mth layer. The discrepancy between the sharpness of the observed and calculated reflexions shows that $\bar{m}$ must be increased by 2–3 units, and since the reflexions have not been corrected for instrumental broadening the upper value is the more likely.

Columns (2), (3) and (4) of Table 2 show the positions of the maxima of the calculated reflexions from Fig. 2, the corresponding apparent value of b (assuming $b_{\text{true}} = 9{\cdot}24$ Å) and the observed values of $b_{\text{app.}}$. In the case of 011, 013, 033 and 060, the position of the main peak in the contribution from the mth layer is a monotonic function of m. One may therefore consider the calculated reflexion to correspond to an 'equivalent value of m' for a single layer, and so deduce the change in this value required to bring the calculated and observed values of $b_{\text{app.}}$ into agreement. The best agreement is obtained if the 'equivalent value of m' is increased by about 3·5. It may be deduced at the same time that the assumed value of b_{true} (9·24 Å) is correct to within about ±0·02 Å. The values of $b_{\text{app.}}$ resulting from this adjustment are shown in column (5) of Table 2. It is not possible to apply similar considerations to 031 and 062 since the position of the main peak of the mth layer is not a monotonic function of m, but the effects of the adjustment on these reflexions may be expected to be small and favourable.

Table 2

		b_{apparent} (Å)		
Reflexion	Position of calculated maximum (k)	Calc. (1st approx.)	Obs.	Calc. (2nd approx.)
(1)	(2)	(3)	(4)	(5)
011	1·08	8·56	8·80	8·72
013	1·075	8·60	8·76	8·79
031	3·135	8·85	8·93	—
033	3·055	9·08	9·07	9·09
060	6·03	9·19	9·19	9·19
062	6·185	8·96	9·01	—

The evidence from both the sharpness and the positions of the reflexions thus leads to the same conclusion that the fibres in the distribution chosen for the calculation of Fig. 2 were about three layers too small. It may therefore be expected that the best agreement of observed and calculated profiles will be obtained if the values of m are increased by 3 and the dispersion of m values is kept fairly similar. This is achieved approximately if the parameters m_0 and t are changed to 12 and 20 respectively. Insertion of these values in (3) gives the corresponding frequency distribution of individual layers. In practice we are more interested in the distribution of fibril size which this implies. It may readily be shown that (3) leads to values

$${}_{O}P_m = \prod_{m_0}^{m} \exp\left\{-tm\left(\frac{1}{m}-\frac{1}{m_0}\right)^2\right\} - \prod_{m_0}^{m+1} \exp\left\{-tm\left(\frac{1}{m}-\frac{1}{m_0}\right)^2\right\}$$

and

$${}_{I}P_m = \prod_{m}^{m_0} \exp\left\{-tm\left(\frac{1}{m}-\frac{1}{m_0}\right)^2\right\} - \prod_{m-1}^{m_0} \exp\left\{-tm\left(\frac{1}{m}-\frac{1}{m_0}\right)^2\right\}$$

for the frequencies of fibrils of which the mth layer is respectively the outermost and innermost. The frequency distributions of fibril diameters for $m_0 = 12$ and $t = 20$ is shown in Fig. 3(a), and the corresponding frequency distribution of fibrils as a function of the number of layers in the tube wall is shown in Fig. 3(b). According to this model the fibrils most commonly have internal and external diameters of about 110 Å and 260 Å, with 10 layers in the tube wall. The cross-section of such a fibre is depicted in Fig. 4.

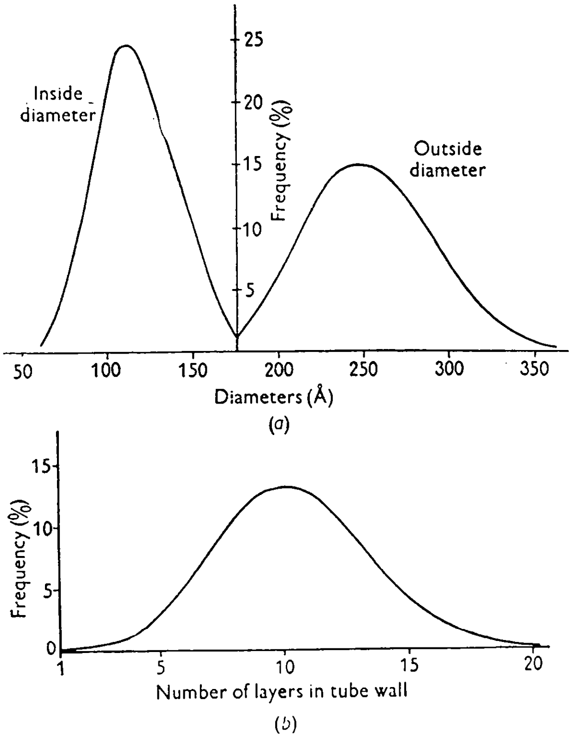

Fig. 3. (a) Frequency distributions of the inside and outside diameters of fibrils which lead to satisfactory agreement of the observed and calculated profiles of the diffuse reflexions. The distributions are based on the assumption that they arise from an exponential function of the strain energy involved in the curvature of the layers. (b) The frequency distribution of fibrils as a function of the number of layers in the tube wall, corresponding to the diameter distributions shown in (a).

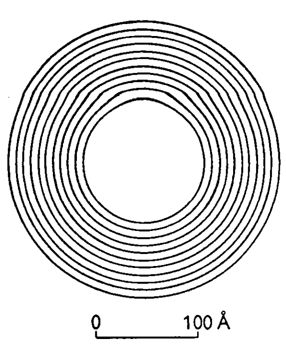

Fig. 4. Cross-section of the most frequently occurring fibril according to the frequency distributions shown in Fig. 3(a).

It would also be possible to determine the average number of layers in the tube wall from the breadth of the $h0l$ reflexions (Whittaker, 1954). This has not been done owing to the difficulty of making a reliable correction for the instrumental broadening in a fibre photograph, but the above value is in satisfactory qualitative agreement with the breadth observed.

It may be noted that the strain-free layer in the distribution deduced above has a radius of 88 Å. This value is in excellent agreement with the radius of the corrugated layer of the same composition in antigorite, for which a value of 85±5 Å has been suggested by Zussman (1954). Also, the mean radius of the most frequently occurring fibre (92 Å) is in good agreement with the value of 84 Å deduced from the position of the helical $\bar{1}06$ reflexion of clinochrysotile (Whittaker, 1956a) and the value of 97 Å similarly deduced from the position of the 060 reflexion of para-chrysotile (Whittaker, 1956c).

7. General conclusions

It has been shown in § 4 that there is evidence that chrysotile contains at least a proportion of bounded layers, but it is not possible to decide, on the basis of diffraction by macroscopic specimens, whether this is due to spiral cylinders or to layers in the form of cylindrical arcs. Such a distinction is possible in principle from the diffraction of single fibrils, but has not yet been achieved in practice. However, it is possible to adduce a considerable amount of circumstantial evidence on the matter.

Jagodzinski & Kunze (1954a) have suggested that the difficulty of nucleation would make it unlikely that a second layer would grow on any layer which had grown in the form of a circular cylinder, and they therefore conclude that all multi-layer fibrils must be spiral. This is certainly a persuasive argument but it loses much of its force without the assumption that the unit cell in the cylindrical projection down [010] contains only one layer; for, if this projection contains two layers, even a spiral cylinder must have been formed as a result of a second nucleation on the layer which was first formed. Since it is now established (Whittaker & Zussman, 1956) that there are two layers in the unit cell, the question of circular or spiral character must be regarded as reopened. Moreover, there is evidence that, in some specimens at least, the circular cylindrical form must predominate. These are the specimens (Whittaker, 1953) in which there is marked disorder of the layers parallel to the fibre axis. Such disorder would not be expected to occur in a spiral cylindrical structure, in which every alternate layer would be part of the same sheet of atoms.

If the structure is based on a circular cylindrical lattice it is necessary (Whittaker, 1955c) that $nb = 2\pi a'$, where a' is the radial spacing of the layers (exactly so if the lattice is regular, and within 0·05 % if it is helical). The value of b should therefore be 9·19 Å (with $n = 5$), whereas the value deduced in § 6 was 9·24 Å. This difference is not sufficiently large to cause the hypothesis of a circular cylindrical lattice to be rejected, however. The observed value of 9·24 Å is based on the supposition that the neutral surface of the chrysotile layer with respect to bending passes through O_3. If this is not true, 9·24 Å will correspond to an average value of b_{m,O_3}, whereas the theoretical value of 9·19 Å corresponds to the true value of b on the neutral surface wherever that may be. The two values could be reconciled if the neutral surface were assumed to lie at a radius about 0·5 Å less than that assumed; i.e. at a level about 30% of the way from O_3 to Si.

The two possible major objections to a circular, as opposed to a spiral, cylindrical structure can therefore be overcome, and there is circumstantial evidence in favour of it in a small number of specimens. However, the question of circular or spiral character must be left open so far as the normal fibrils from the majority of sources are concerned.

Pundsack (1956) has recently shown that the density of sealed blocks of chrysotile is too high to admit of the presence of the voids which would be involved in a packing of parallel hollow cylindrical fibres. Such an arrangement consisting wholly of fibrils of the dimensions suggested in § 6 would contain 25% voids (inter-fibrillar voids 9%; intra-fibrillar voids 16%). Pundsack therefore proposes that the layers composing the fibrils must be in the form of cylindrical arcs, not complete cylinders. Pundsack does not resolve the difficulty of reconciling this suggestion with the cylindrical appearance of chrysotile fibres in electron micrographs. It may also be urged that the existence of a helical structure in clino-chrysotile and para-chrysotile (Whittaker, 1956*a*, *c*), in which the parameters found are those required for an advance of one unit cell along the axis for a complete turn of the helix, is good evidence that the cylinders must be complete. It seems probable that the density evidence can be reconciled with the X-ray and electron microscope evidence if it is assumed (*a*) that the inter-fibrillar voids are filled by layers in the form of cylindrical arcs coaxial with the adjacent fibres, and (*b*) that the intra-fibrillar voids are usually filled by layers in the form of cylindrical arcs oriented parallel to, but not coaxial with, the walls of the fibre, but a small proportion of the fibres are hollow.

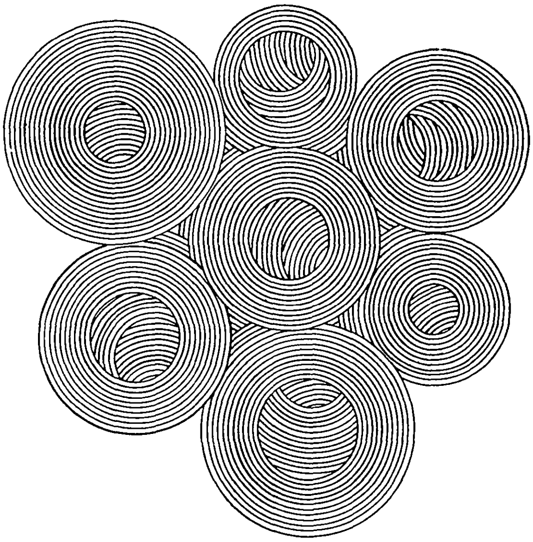

Fig. 5. Cross-section of a packing of fibrils in which both the inter-fibrillar and intra-fibrillar voids are filled by layers in the form of cylindrical arcs.

A cross-section of a packing of fibres of this form is shown in Fig. 5. If the proportion of hollow fibres were of the order of 5%, this would involve a discrepancy of only 0·02 between the observed and calculated values of the specific gravity, which would seem to be reconcilable with Pundsack's evidence. At the same time 75% of the material would be in the form of complete cylinders (which would be reconcilable with the preponderance of helical fibres in Thetford chrysotile), and the remainder would provide the material with layer boundaries which has been postulated in § 4 above. The electron microscope evidence could also be explained if it were assumed that the preparation of the specimens for electron microscopy (by evaporation of a dilute aqueous suspension after the heavier particles have settled) tends to concentrate the hollow fibres. In this connection it is perhaps worth while to point out that synthetic chrysotile (Noll & Kircher, 1950, 1951) appears more definitely and uniformly tubular in electron micrographs than do many specimens of natural chrysotile, and the synthetic material may reasonably be supposed to be entirely in the form of hollow tubes.

I wish to thank the Directors of Ferodo Ltd for permission to publish this paper.

This work forms part of a thesis accepted by the University of London for the degree of Ph.D.

References

Aruja, E. (1943). Ph.D. Thesis, Cambridge.

Jagodzinski, H. & Kunze, G. (1954*a*). *N. Jb. Miner. Mh.* p. 113.

Jagodzinski, H. & Kunze, G. (1954*b*). *N. Jb. Miner. Mh.* p. 137.

Jahnke, E. & Emde, F. (1952). *Tables of Higher Functions*, 5th ed. Leipzig: Teubner.

Noll, W. & Kircher, H. (1950). *Naturwissenschaften*, **37**, 540.

Noll, W. & Kircher, H. (1951). *N. Jb. Miner. Mh.* p. 219.

Pundsack, F. L. (1956). *J. Phys. Chem.* **60**, 361.

Whittaker, E. J. W. (1953). *Acta Cryst.* **6**, 747.

Whittaker, E. J. W. (1954). *Acta Cryst.* **7**, 827.

Whittaker, E. J. W. (1955*a*). *Acta Cryst.* **8**, 261.

Whittaker, E. J. W. (1955*b*). *Acta Cryst.* **8**, 265.

Whittaker, E. J. W. (1955*c*). *Acta Cryst.* **8**, 571.

Whittaker, E. J. W. (1955*d*). *Acta Cryst.* **8**, 726.

WHITTAKER, E. J. W. (1956*a*). *Acta Cryst.* **9**, 855.
WHITTAKER, E. J. W. (1956*b*). *Acta Cryst.* **9**, 862.
WHITTAKER, E. J. W. (1956*c*). *Acta Cryst.* **9**, 865.
WHITTAKER, E. J. W. & ZUSSMAN, J. (1956). *Miner.Mag.* **31**, 107.
ZUSSMAN, J. (1954). *Miner. Mag.* **30**, 498.

Acta Cryst. (1957). **10**, 156

The Crystal Structure of P_4S_5

BY S. VAN HOUTEN AND E. H. WIEBENGA

Laboratorium voor Anorganische en Fysische Chemie der Rijksuniversiteit, Groningen, Netherlands

(*Received* 14 *September* 1956)

The crystal structure of P_4S_5 has been determined by X-ray diffraction. Space group $P2_1$, 2 molecules per unit cell. Approximate coordinates were found from a three-dimensional Patterson synthesis. The coordinates were refined by means of successive Fourier syntheses of the three projections. The crystal consists of molecules of P_4S_5, which have an unexpected structure. The P–S distances vary from 2·08 to 2·19 Å, the average P–P distance is 2·21 Å and the P=S distance is 1·94 Å.

Introduction

Phosphorus and sulphur form the compounds P_4S_3, P_4S_5, P_4S_7 and P_4S_{10} (Stock, 1910; Treadwell & Beeli, 1935; Pernert & Brown, 1949). The structures of these compounds have been investigated in our laboratory during recent years (Vos & Wiebenga, 1955; van Houten, Vos and Wiegers, 1955); that of P_4S_3 has also been determined independently by Leung, Waser & Roberts (1955). The structure determination of P_4S_5, being the last compound investigated, is described in the present paper.

Experimental

Materials

P_4S_5 is formed when a solution of P_4S_3, sulphur and some iodine in dry carbon disulphide is exposed to diffuse daylight for three days (Boulouch, 1904). The reaction has to take place in a closed vessel in an atmosphere of carbon dioxide to prevent the oxidation of P_4S_3. The substance can be purified by recrystallization from carbon disulfide. The X-ray photographs were made from crystals having a diameter of approximately 0·1 mm. perpendicular to the axis about which the photographs were taken. The crystals were mounted in capillaries of borosilicate glass.

Space group and lattice constants

Weissenberg photographs showed the crystals to be monoclinic. The systematic absences are those required by the space groups $P2_1$ or $P2_1/m$. The pyroelectricity of the crystals indicated the space group $P2_1$, which was confirmed by the result of the structure determination.

The lattice constants were measured on Weissenberg and oscillation photographs about the three axes. With $\lambda(\text{Cu } K\alpha) = 1{\cdot}5418$ Å the following values for the lattice constants were obtained:

$$a = 6{\cdot}41 \pm 0{\cdot}03,\quad b = 10{\cdot}94 \pm 0{\cdot}04,\quad c = 6{\cdot}69 \pm 0{\cdot}03 \text{ Å},\quad \beta = 111{\cdot}7 \pm 0{\cdot}4^\circ .$$

The inaccuracies listed are estimated standard deviations. With two molecules per unit cell the density was calculated to be 2·15 g.cm.$^{-3}$; the experimental value is 2·17 g.cm.$^{-3}$ at 25° C. (Treadwell & Beeli, 1935).

Structure factors

The intensities of 738 independent reflexions hkl were estimated visually on equi-inclination Weissenberg photographs about the a axis, using Ni-filtered Cu radiation. Use was made of the multiple-film technique. The crystals were twins with common b^* and c^* axes; therefore two sets of reflexions were available on all but the zero layer lines. A correction for absorption was applied. The intensity data observed on different layer lines were related by $h0l$ and $hk0$ reflexions from integrated equiinclination Weissenberg photographs (Wiebenga & Smits, 1950) about the b and c axes respectively. In the course of the structure determination the scale factors thus obtained were somewhat adjusted, using the calculated structure factors.

Determination of the structure

Interpretation of the Patterson synthesis

After some unsuccessful attempts to solve the structure by means of inequalities, a three-dimensional Patterson synthesis was computed. Peaks around the origin at distances of about 2 Å give the vectors between bonded atoms. These peaks were all very low,